Directional exciton-polariton photoluminescence emission from terminals of a microsphere-coupled organic waveguide

Ravi P. N. Tripathi, Rohit Chikkaraddy, Arindam Dasgupta, and G. V. Pavan Kumar

Citation: Appl. Phys. Lett. **108**, 031102 (2016);
View online: https://doi.org/10.1063/1.4939980
View Table of Contents: http://aip.scitation.org/toc/apl/108/3
Published by the American Institute of Physics

Directional exciton-polariton photoluminescence emission from terminals of a microsphere-coupled organic waveguide

Ravi P. N. Tripathi, Rohit Chikkaraddy,[a] Arindam Dasgupta, and G. V. Pavan Kumar[b]
Photonics and Optical Nanoscopy Laboratory, Physics Division and Center for Energy Science, h-cross, Indian Institute of Science Education and Research, Pune 411008, India

(Received 13 November 2015; accepted 5 January 2016; published online 19 January 2016)

We report on angle-resolved, exciton-polariton photoluminescence measurements from asymmetric terminals of a microsphere-coupled organic waveguide (MOW). The MOW architecture consisted of a SiO_2 microsphere coupled with a diaminoanthroquinone mesowire, self-assembled on a glass substrate. The angle-resolved emission measurements were performed using spatially filtered Fourier-plane optical imaging method. The light emanating from the sphere-terminus had two regions of angular emission in the Fourier-plane, of which one had azimuthal angular spread as small as 10°. The emission from wire terminus was uni-directional in nature, with some light emitted beyond the critical angle of glass-air interface. Our results highlight unique directional emission characteristics of a hybrid organic waveguide geometry and may have implications on single-element, exciton-polariton based light-emitting devices and lasers. © *2016 AIP Publishing LLC*. [http://dx.doi.org/10.1063/1.4939980]

There is a high demand for materials which can be adapted to realize devices that are inexpensive, flexible, and clean. Organic molecular materials cater to this requirement and have been extensively studied in the context of photovoltaics and opto-electronics.[1–11] In recent years, organic nanomaterials have also been explored in the context of nanophotonics, where light has to be managed at subwavelength scales.[1,11–21] Specifically, organic semiconductor materials have been under exploration as they facilitate exciton-polaritons (EPs), which are essentially quasiparticles of matter and light. The EPs in organic materials arise due to the coupling of Frenkel excitons with electromagnetic radiation[1] and have been extensively studied both in the context of fundamental physics and technological applications.[1,22–25] Compared to Wannier-Mott excitons in inorganic materials,[25,26] Frenkel EPs have advantage of higher exciton binding energy, larger oscillator strength, high photoluminescence, and greater stability which further helps in guiding photons at subwavelength scale with minimal losses.[1,22,27–33] Recently, EP based organic molecular waveguides have been coupled to optical resonator structures such as microspheres and micro-discs.[30,34,35] Such coupling is motivated to realize active light sources (lasers and light emitting devices), with large quality factors and minimal coupling losses.[34–37] An unexplored aspect of such coupling is the directionality of light emitted from the terminals of such hybrid architectures. This will be crucial factor to further optimize the active emission devices, and also understand how the out-coupled light can be routed and coupled to other structures on a photonic chip.

Motivated by the above requirement, herein we report on characterization of non-reciprocal angular exciton-polariton emission from the terminals of a hybrid meso-architecture: dielectric microsphere coupled organic mesowire waveguide. The dielectric microsphere that we use is of SiO_2 and the organic molecular mesowire is made of diaminoanthroquinone (DAAQ).

A detailed protocol to prepare such hybrid structures can be found in our previous report.[34] Figure 1(a) shows an optical image of a microsphere-coupled organic waveguide (MOW) structure resting on glass substrate. The scanning electron microscopy (SEM) image of the same structure has been shown in Figure 1(b). The insets in Figure 1(b) show higher resolution SEM images of the end terminus of the MOW structure. All the measurements reported in this paper were performed on the MOW structure shown in Figure 1(b). The SEM images in Figures 1(c)–1(f) show a variety of MOW structures, indicating repeatability of our preparation method.

To probe the directionality of EP emission from end terminals of the described geometry, we performed angle-resolved emission measurements in two different

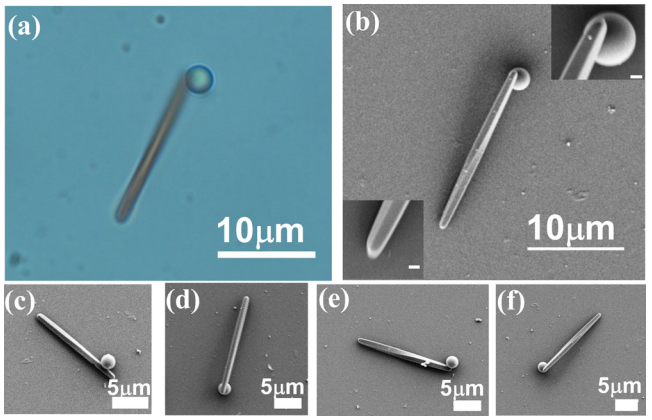

FIG. 1. Microsphere (diameter: 3 μm)-coupled organic waveguide (MOW) on a glass substrate. (a) Optical and (b) scanning electron microscopy (SEM) image of the same MOW structure. Insets show higher resolution SEM images of the two terminals of the architecture. The scale bar for the insets is 500 nm. (c)–(f) SEM images of a variety of isolated MOW structures.

[a]Current Address: Cambridge University, University of Cambridge, Cambridge, CB3 0HE, UK.
[b]Electronic mail: pavan@iiserpune.ac.in

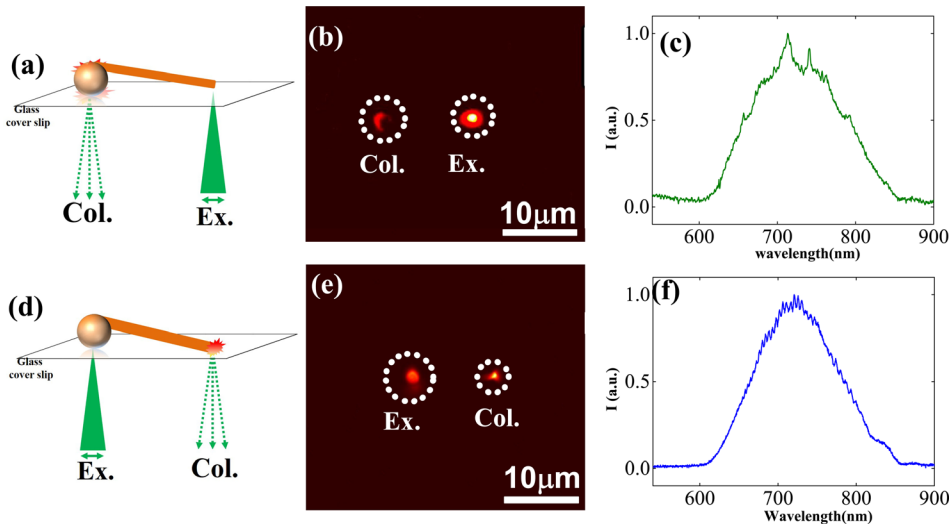

FIG. 2. Two experimental configurations used in this study. (a) Schematic of the first configuration in which free end of the wire was excited (Ex.) and the photoluminescence emission was collected (Col.) from the sphere terminus. (b) Photoluminescence image and (c) spatially filtered photoluminescence spectra from the sphere terminus. (d) Schematic of the second configuration in which sphere terminus was excited and emission was collected from the wire terminus. (e) Photoluminescence image and (f) spatially filtered photoluminescence spectra from the wire end. The excitation source was a 532 nm laser. For photoluminescence imaging and spectroscopy, an edge filter was used to reject the elastic scattered light.

configurations. In Figure 2(a), we show schematic of first configuration where the wire-end was excited with a 532 nm laser using an objective lens (100×, 1.3 NA). This excitation leads to EPs in the mesowire, which further propagate along its length and out-coupled as photoluminescence (PL) from the sphere-terminus. The light emanating from the collection points was spatially filtered (see dotted circle in Figure 2(b)) and routed towards spectrometer to obtain the PL spectra (Figure 2(c)). In Figure 2(d), we show schematic of the second configuration: sphere terminus being excited and the PL were collected from wire-end. The corresponding PL image and PL spectra from the wire terminus are shown in Figures 2(e) and 2(f), respectively. A comparison of whispering gallery mode spectra for various excitation and collection configuration and the related discussion can be found in the supplementary material,[38] Figure S2.

The main objective of these experiments was to analyse the directionality of the emitted PL signal from the collection points shown in Figures 2(b) and 2(e). A home built photoluminescence microscopy with spectroscopic detection and Fourier-plane (FP) imaging capability was utilized, whose details can be found elsewhere.[39,40] For the angle-resolved PL measurements, we projected spatially filtered PL signal from the terminus of MOW structure on the back-focal plane or Fourier-plane (FP) of the objective lens and imaged it on EM-CCD camera (Andor iXon Ultra). The FP images reveal directionality of the PL intensity as a function of two angle θ and ϕ, where θ is the polar angle defined by the numerical aperture of the objective lens (in our case, $0 < \theta < 60^\circ$) and ϕ is the azimuthal angle ($0 < \phi < 360^\circ$).

Configuration 1—Wire excitation, sphere-terminus collection: Figure 3(a) shows the schematic of the experimental configuration with the corresponding projection of emission into the Fourier plane. In Figure 3(b), we show the intensity distribution as a function of angles θ and ϕ. The emission was pronounced at two values of polar angles $\theta = 40^\circ$ and 30°. Figure 3(c) shows intensity as a function of ϕ at $\theta = 40^\circ$. The dominant emission was around $\phi = 240^\circ$, with an azimuthal spread ($\delta\phi$) of around 60°. Such high forward-to-backward ratio in the angular emission pattern is similar to the case of

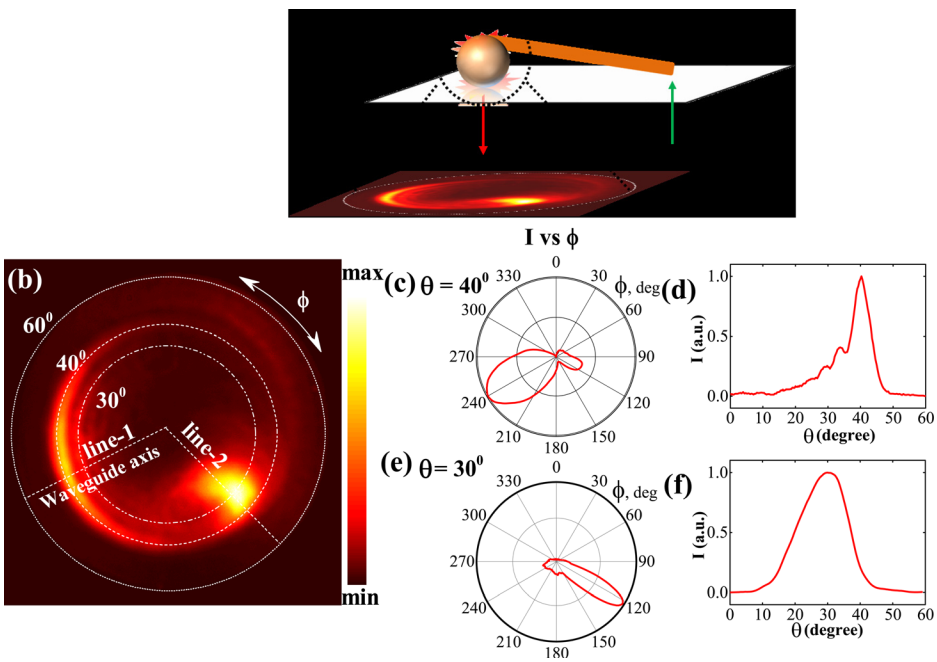

FIG. 3. (a) Schematic of the excitation and emission configuration, and the Fourier-plane (FP) projection of the emitted light. (b) FP image of the intensity of the emitted light from the sphere terminus of MOW structure. The outer most circle ($\theta = 60^\circ$) represents the angle of numerical aperture of the objective lens (100×, 1.3 NA). (c) Intensity distribution as a function of azimuthal angle (ϕ) for $\theta = 40^\circ$ (close to critical angle of glass-air interface). (d) Intensity distribution as a function of polar angle (θ) for the line 1 shown in Figure 3(a). (e) Intensity distribution as a function of ϕ for $\theta = 30^\circ$. (f) Intensity distribution as a function of θ for line 2 shown in Figure 3(a).

plasmonic nanowires,[39] and an interesting feature to note in our results. In Figure 3(c), we also observed a weak emission around $\phi = 120°$, with an azimuthal spread of around 30°. Figure 3(d) shows intensity distribution as a function of θ along line 1 (shown in Fig. 3(a)). The maximum intensity measured was at around 40°, which is close to the critical angle of glass-air interface (41.5°) and represents out-coupling of leaky waves.[39] Interestingly, the intensity distribution was oscillatory in nature for θ value less than 40°. The oscillatory intensity distribution indicates various waveguide modes being channelled at different polar angles. Such oscillatory emission patterns have been observed in complex plasmonic waveguide geometries.[41] Our observation is unique in the sense that such oscillatory intensity distribution has been observed for a hybrid organic waveguides. Furthermore, in order to show the importance of wire-excitation sphere-collection configuration, we compared the angle-resolved emission with sphere-excitation sphere-collection configuration (see the supplementary material,[38] Figure S1 and the related discussion) and found that only in case of the former we obtain directional emission. This further highlights the relevance of MOW structure in the context of directional photoluminescence emission.

Figure 3(e) shows intensity distribution as a function of ϕ at $\theta = 30°$. We observed sharp directionality with respect to ϕ with an azimuthal spread as small as 10°. However, the spread in θ along line 2 (see Fig. 3(a)) was large as shown in Figure 3(f), with the intensity peaking at $\theta = 30°$. The origin of this highly directional emission may be due to the direct leakage of exciton-polaritons from the sphere-glass interface. The light emitted from the wire is channelled into the glass substrate. Upon recording the emission through the glass and projecting it into the Fourier plane, we obtain pronounced intensity distribution in two regions of the Fourier plane (Figure 3(b)). The first region is represented by the arc-like emission. This emission is due to directional out-coupling of light from the distal end of mesowire. The second region is represented by a bright spot in the Fourier plane. This small angular distribution may be attributed to the focusing effect of the microsphere. Such confined angular distribution suggests a kind of converging-lens effect, probably due to photonic jets[42–44] (a 3D finite difference time domain model and discussion of the photonic jet effect and its dependence on angle of excitation can be found in the supplementary material,[38] Figure S4).

The obtained angular emission is sensitive to parameters such as coupling configuration, coupling distance between microsphere and organic waveguide, size and geometry of microsphere, and waveguide cross-section. Therefore, its angular emission can be tuned by precisely controlling these parameters. To ascertain the repeatability of our results, directional emission study on two different MOW structures were performed, whose results are shown in the supplementary material[38] (see Figures S1(ii) and S3).

Configuration 2—Sphere excitation, wire-terminus collection: Figure 4(a) shows the schematic of the optical configuration where the sphere was excited, and the optical emission was spatially filtered from the wire terminus of the MOW structure, and further projected on to the Fourier plane. Figure 4(b) shows the intensity distribution of the

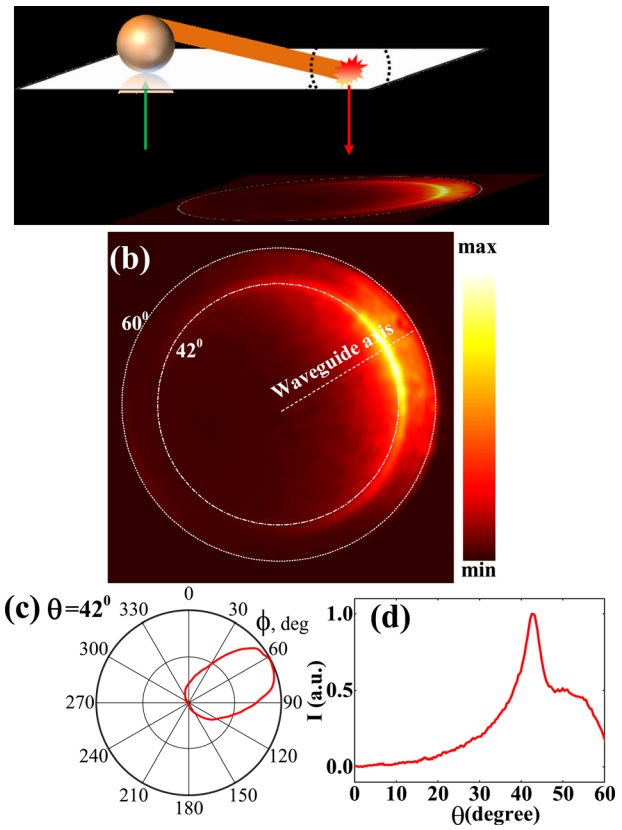

FIG. 4. (a) Schematic of the sphere-excitation and wire-emission configuration, and the Fourier-plane (FP) projection of the emitted light from distal end of the mesowire. (b) FP image of the intensity of the emitted light from the wire terminus of MOW structure. (c) Intensity distribution as a function of ϕ for $\theta = 42°$. (d) Intensity distribution as a function of θ for the line shown in Figure 3(b).

emitted light as a function of ϕ and θ. The emitted light was directional in nature, with majority of the emission occurring at the $\theta = 42°$. We also observed some emission beyond this angle, upto $\theta = 60°$. We further quantified the emission by resolving it as a function of ϕ for $\theta = 42°$, as shown in Figure 4(c). We found azimuthal angular spread greater than 60°, which was much greater than the case for sphere terminus emission (see Figure 3(c)). Figure 4(d) shows the distribution of intensity as a function of θ for the dotted line shown in Figure 4(b). We found maximum emission for $\theta = 42°$, which was at the critical angle of the glass-air interface. Interestingly, we found some emission beyond the critical angle, which was in contrast to the sphere-terminus emission (see Figure 3(d)). It is to be noted that the dependence of θ on effective refractive index can be further harnessed as a refractive index sensor as show recently.[39] Such emission beyond critical angle has also been observed in fluorescence of dye molecule at a dielectric interface[45] and depends on the geometrical factors of the emitter with respect to the substrate. In our case, the wire orientation may also have some connection to the emission beyond critical angle.

To summarize, we have studied angle dependent exciton-polariton emission from the two terminus of an MOW structure placed on a glass substrate. Our analysis of the angular emission from the sphere terminus revealed two regions of directional emission, of which one of them had an

azimuthal spread as small as 10°. For the wire-terminus emission, the angular spread had a greater azimuthal spread (>60°), with emission leaking beyond critical angle of glass-air interface. Our experiments indicate how angular emission varies when the light is collected at two different terminus of a hybrid waveguide: MOW structure. The directionality of light, especially from the sphere terminus, should have direct implication on directional light emitted devices, including one-dimensional exciton-polariton based laser. It would be interesting to extrapolate our work to observe angle-resolved nonlinear optical emission from two terminus of the MOW structure. Such studies may facilitate nanophotonic platforms to control and direct light at sub-wavelength scale.

This research work was partially funded by DST-Nanomission Grant (SR/NM/NS-1141/2012(G)) and DST Nanoscience Unit Grant (SR/NM/NS-42/2009), India. R.C. wishes to acknowledge financial support from KVPY fellowship.

[1]Y. S. Zhao, *Organic Nanophotonics* (Springer, 2015).
[2]Z. R. Li, *Organic Light-Emitting Materials and Devices* (CRC Press, 2015).
[3]D. Konios, C. Petridis, G. Kakavelakis, M. Sygletou, K. Savva, E. Stratakis, and E. Kymakis, Adv. Funct. Mater. **25**, 2206–2206 (2015).
[4]Y. S. Zhao, H. Fu, A. Peng, Y. Ma, Q. Liao, and J. Yao, Acc. Chem. Res. **43**, 409–418 (2010).
[5]R. Chandrasekar, Phys. Chem. Chem. Phys. **16**, 7173–7183 (2014).
[6]F. S. Kim, G. Ren, and S. A. Jenekhe, Chem. Mater. **23**, 682–732 (2011).
[7]S. K. Saikin, A. Eisfeld, S. Valleau, and A. Aspuru-Guzik, Nanophotonics **2**, 21–38 (2013).
[8]J. Kjelstrup-Hansen, C. Simbrunner, and H.-G. Rubahn, Rep. Prog. Phys. **76**, 126502 (2013).
[9]T. Kim, L. Zhu, R. O. Al-Kaysi, and C. J. Bardeen, ChemPhysChem **15**, 400–414 (2014).
[10]M. Schiek, F. Balzer, K. Al-Shamery, J. R. Brewer, A. Lützen, and H.-G. Rubahn, Small **4**, 176–181 (2008).
[11]F. Quochi, J. Opt. **12**, 024003 (2010).
[12]J. Xu, S. Semin, T. Rasing, and A. E. Rowan, Small **11**, 1113–1129 (2015).
[13]W. Yao, G. Han, F. Huang, M. Chu, Q. Peng, F. Hu, Y. Yi, H. Jiang, J. Yao, and Y. S. Zhao, Adv. Sci. **2**, 1500130 (2015).
[14]F. Balzer, V. G. Bordo, A. C. Simonsen, and H.-G. Rubahn, Phys. Rev. B **67**, 115408 (2003).
[15]S. Basak and R. Chandrasekar, J. Mater. Chem. C **2**, 1404–1408 (2014).
[16]N. Chandrasekhar, M. A. Mohiddon, and R. Chandrasekar, Adv. Opt. Mater. **1**, 305–311 (2013).
[17]K. Takazawa, J.-I. Inoue, K. Mitsuishi, and T. Takamasu, Phys. Rev. Lett. **105**, 067401 (2010).
[18]K. Takazawa, J.-I. Inoue, K. Mitsuishi, and T. Takamasu, Adv. Mater. **23**, 3659–3663 (2011).
[19]F. Balzer, V. Bordo, A. C. Simonsen, and H.-G. Rubahn, Appl. Phys. Lett. **82**, 10–12 (2003).
[20]F. Balzer and H.-G. Rubahn, Appl. Phys. Lett. **79**, 3860 (2001).
[21]F. Balzer and H.-G. Rubahn, Adv. Funct. Mater. **15**, 17–24 (2005).
[22]Y. Yan and Y. S. Zhao, *Soft Matter Nanotechnology: From Structure to Function* (Wiley-VCH, 2015), pp. 131–160.
[23]S.-Y. Min, T.-S. Kim, Y. Lee, H. Cho, W. Xu, and T.-W. Lee, Small **11**, 45–62 (2015).
[24]J. Yang, D. Yan, and T. S. Jones, Chem. Rev. **115**, 5570–5603 (2015).
[25]C. J. Bardeen, Ann. Rev. Phys. Chem. **65**, 127–148 (2014).
[26]J. J. Piet, P. N. Taylor, B. R. Wegewijs, H. L. Anderson, A. Osuka, and J. M. Warman, J. Phys. Chem. B **105**, 97–104 (2001).
[27]M. Zamfirescu, A. Kavokin, B. Gil, G. Malpuech, and M. Kaliteevski, Phys. Rev. B **65**, 161205 (2002).
[28]Y. S. Zhao, J. Xu, A. Peng, H. Fu, Y. Ma, L. Jiang, and J. Yao, Angew. Chem. **120**, 7411–7415 (2008).
[29]C. Zhang, C.-L. Zou, Y. Yan, R. Hao, F.-W. Sun, Z.-F. Han, Y. S. Zhao, and J. Yao, J. Am. Chem. Soc. **133**, 7276–7279 (2011).
[30]C. Zhang, Y. S. Zhao, and J. Yao, Phys. Chem. Chem. Phys. **13**, 9060–9073 (2011).
[31]K. Takazawa, Chem. Phys. Lett. **452**, 168–172 (2008).
[32]H. Yanagi and T. Morikawa, Appl. Phys. Lett. **75**, 187–189 (1999).
[33]T. Yokoyama, Appl. Phys. Lett. **96**, 063101 (2010).
[34]R. Chikkaraddy, A. Dasgupta, S. D. Gupta, and G. V. P. Kumar, Appl. Phys. Lett. **103**, 031112 (2013).
[35]C. Wei, S.-Y. Liu, C.-L. Zou, Y. Liu, J. Yao, and Y. S. Zhao, J. Am. Chem. Soc. **137**, 62–65 (2015).
[36]Y. Dong, K. Wang, and X. Jin, Opt. Commun. **350**, 230–234 (2015).
[37]Y. Dong, K. Wang, and X. Jin, Appl. Opt. **54**, 277–284 (2015).
[38]See supplementary material at http://dx.doi.org/10.1063/1.4939980 for discussion on directional emission of a microsphere and two different MOW structures with the corresponding FDTD simulations. A brief discussion on WGMs of MOW structures has been provided.
[39]T. Shegai, V. D. Miljkovic, K. Bao, H. Xu, P. Nordlander, P. Johansson, and M. Kall, Nano Lett. **11**, 706–711 (2011).
[40]D. Singh, A. Dasgupta, V. Aswathy, R. P. N. Tripathi, and G. V. Pavan Kumar, Opt. Lett. **40**, 1006–1009 (2015).
[41]L. Zhu, D. Zhang, R. Wang, P. Wang, H. Ming, R. Badugu, L. Du, X. L. Yuan, and J. R. Lakowicz, J. Phys. Chem. C **119**, 24081–24085 (2015).
[42]Z. Wang, preprint arXiv:1509.08031 (2015).
[43]A. Darafsheh, N. I. Limberopoulos, J. S. Derov, D. E. Walker, Jr., and V. N. Astratov, Appl. Phys. Lett. **104**, 061117 (2014).
[44]A. Darafsheh, C. Guardiola, A. Palovcak, J. C. Finlay, and A. Cárabe, Opt. Lett. **40**, 5–8 (2015).
[45]H. H. Choi, H. J. Kim, J. Noh, C.-W. Lee, and W. Jhe, Phys. Rev. A **66**, 053803 (2002).